Journal of Computer Assisted Tomography
19(6):871–878, November/December

3D Phase Contrast EPI MR Angiography of the Carotid Arteries

Simon Wildermuth, Jörg F. Debatin, Thierry A. G. M. Huisman, Daniel A. Leung, and Graeme C. McKinnon

Objective: Our goal was to compare 3D phase contrast (PC) echo planar imaging (EPI) MRA of the carotid and vertebral arteries with conventional 3D PC in volunteers and patients.

Materials and Methods: The carotid arteries of 12 volunteers were imaged with conventional and EPI 3D PC sequences. The visibility for each of seven carotid and four vertebral segments was qualitatively assessed. Signal intensity and homogeneity determinations were performed on the source images. Three patients with known carotid artery disease were also imaged with the same protocol.

Results: EPI reduced 3D PC data acquisition time from 459 to 32 s (factor of 15). Both techniques permitted full assessment of the common carotid artery, the bifurcation, as well as the proximal internal carotid artery (ICA), external carotid artery (ECA), and vertebral arteries. Visualization of the distal ICA/ECA and vertebral arteries was inferior with EPI compared with the conventional acquisition. In all patients, lesions as established by X-ray angiography were seen to equal advantage with both techniques.

Conclusion: EPI 3D PC MRA renders diagnostic images of the proximal carotid system. The considerable reduction in data acquisition time must be weighed against poorer image quality.

Index Terms: Magnetic resonance imaging, angiography (MRA)—Magnetic resonance imaging, techniques—Arteries, carotid—Arteries, vertebral.

Cerebral infarction has been implicated as the third most frequent cause of death in industrialized nations. It is most commonly a fatal manifestation of atherosclerotic disease of the carotid arterial system. Atherosclerotic carotid disease can be treated. In fact, surgical carotid endarterectomy has been shown to significantly reduce the incidence of cerebral infarction (1). Treatment, however, can translate into reduced morbidity and mortality only if the disease process is diagnosed prior to the manifestation of permanent cerebral damage. This has stimulated vast interest in the identification and evaluation of accurate, cost-efficient, and preferably noninvasive diagnostic screening modalities.

Conventional cerebral angiography to date remains the gold standard for the pre-operative evaluation of the carotid system. This method, however, is invasive, requires the application of intravascular contrast agents, and is associated with a small yet measurable (1–4%) incidence of complications including transient ischemic attacks and even cerebral infarction (2). Furthermore, this examination is both time and cost intensive and thus not well suited for screening purposes.

MR angiography (MRA) has been shown to be useful in the evaluation of the carotid arterial system (3–7). In fact, a recent study of endarterectomy specimens has shown that MRI might actually reflect complex vascular morphology in the region of the carotid bifurcation more accurately than conventional arteriography (8). MRA is totally noninvasive, is not associated with any known side effects, and can easily be performed as an outpatient examination. A sufficiently high level of diagnostic accuracy mandates excellent image quality and hence high image resolution.

Conventional MRI requires a separate MR exper-

From the Department of Radiology–MRI Center, University Hospital Zurich, Rämistrasse 100, CH-8091 Zurich, Switzerland. Address correspondence and reprint requests to Dr J. F. Debatin.

iment for each line in k-space, resulting in lengthy imaging times between 10 and 30 min (9). Beyond the monetary cost associated with such lengthy acquisition times, the technique is prone to motion artifacts induced by minimal patient motion or swallowing. These are capable of severely degrading image quality and have been shown to obscure disease as well as simulate lesions in regions of normal vascular morphology.

Through the implementation of stronger and faster gradient systems, ultrafast echo planar imaging (EPI) strategies, as first described by Mansfield (10), now appear practical. These allow vast reductions of MR data acquisition times.

Echo planar data acquisition schemes can be applied to MRA (11–13). The purpose of the study was to evaluate an ultrafast EPI MRA with regard to its ability to depict the carotid arterial morphology. We present the initial implementation of a 3D multishot EPI gradient-recalled echo (GRE) phase contrast (PC) sequence that combines ultrafast data acquisition with adequate spatial resolution to depict sufficient vascular detail. Following assessment of this ultrafast imaging strategy with respect to conventional MRA in normal subjects, the performance of the technique was evaluated in three patients in a comparison with conventional contrast angiography as well as conventional MRA.

SUBJECTS AND METHODS

Subjects

MRA examinations of both carotid arterial systems were performed on 12 normal subjects (8 men, 4 women) and 3 patients. Informed consent was obtained from each subject as mandated by our institutional review board. The volunteers, aged between 24 and 36 years (mean age 27.4 years), had no evidence of arterial disease. All patients (two men, one woman), aged between 65 and 78 years, had undergone conventional contrast angiography for the evaluation of clinically suspected severe atherosclerotic changes in the carotid arteries. Selective cerebral angiography was performed with a femoral artery approach. Biplane film screen imaging in the anteroposterior and lateral projections was performed in conjunction with digital subtraction angiographic imaging.

MRI

All studies were performed on a 1.5 T MR scanner (Signa; GE Medical Systems, Milwaukee, WI, U.S.A.), equipped with a prototype gradient configuration in the x-axis for nonresonant EPI (slew rate 200 mT/m/ms, amplitude 18 mT/m, ramp time 90 μs).

3D PC MRA examinations of the carotid arteries were performed on all subjects based on conventional as well as echo planar data acquisition strategies. To enhance image quality, all MRA examinations were performed with a surface coil (anterior neck coil) for signal reception. The subjects were instructed to minimize any head or swallowing motion while data acquisition was ongoing.

Based on sagittal localizing images, a 15 cm wide imaging volume, consisting of 60 × 2.5 mm sections, was centered on the carotid bifurcation for the 3D PC acquisitions. For the 3D EPI PC measurements, a 2D plane of 3D k-space data was acquired in eight shots. With this acquisition strategy, 10 k-space lines are collected following a single RF pulse. The eight shots were collected in a k-spaced interleaved fashion (14). Positive and negative velocity-encoded measurements were obtained in direct succession. Conventional phase encoding was applied to scan in the third k-space direction. To ensure a steady magnetization state, two successive dummy pulses (shots without data collection) were applied before the actual data acquisition.

The particular choice of imaging parameters was driven by the attempt to provide optimal image quality in the shortest possible data acquisition time. To enable a valid comparison, the number of sections (n = 60), section thickness (2.5 mm), field of view (26 × 13), and imaging matrix (256 × 128) were identical, rendering an in-plane resolution of 1.02 × 1.02 mm and a voxel volume of 2.5 mm^3. Flow was encoded in the superoinferior direction with a velocity-encoding value of 1.2 m/s. A flip angle of 20° was employed for the conventional acquisition; for EPI a flip angle of 25° was used. While the conventional 3D PC data were based on full k-space data acquisition, reconstruction of EPI images was based on a fractional k-space acquisition, collecting 80 k-lines per image. The missing k-lines were zero-filled, and the amplitude of the unpaired lines was scaled by a factor of 2. A conventional 2D Fourier transform was applied and a modulus image was taken.

The EPI data were collected with a sampling rate of 166.6 kHz (6 μs/sample), translating into a minimum effective TE of 9.4 ms and a TR, defined as the time between two successive RF pulses, of 28 ms. For the conventional 3D PC acquisition, a slightly shorter TE of 7.2 ms could be achieved. The minimum TR of 28 ms was identical to that of the echo planar sequence. The sampling rate was 32 kHz.

For reconstruction, the 3D PC data sets were transferred to a SPARC 10 workstation (Sun Microsystems, Mountain View, CA, U.S.A.). Subsequently, the axial 3D images were coronally reconstructed, using a "maximum pixel intensity pro-

jection" algorithm (15), implemented on a commercially available postprocessing program (interactive vascular imaging; GE Medical Systems, Milwaukee, WI, U.S.A.).

Image Analysis

Using the 20th magnitude-weighted PC section of all image sets, signal intensity (SI) measurements covering operator-defined regions of interest were performed in both common carotid arteries (CCAs) as well as in the surrounding tissues not containing flowing spins, hence representing background. Noise was defined as the standard deviation of the SI outside the imaging volume. Vessel signal-to-noise ratios (SNRs), vessel-to-background contrast-to-noise ratios (CNRs), and vessel-to-background SI ratios were calculated.

For the qualitative comparison of the two techniques, each carotid arterial system was subdivided into seven and each vertebral artery into four segments (Fig. 1). An experienced neuroradiologist, blinded to the underlying data acquisition scheme of the particular image set under review, separately classified each segment as either "adequately visible" or "not adequately visible." The criterion of adequate visibility was fulfilled if disease in that particular arterial segment could with certainty be excluded. Image analysis was based on both the coronal reconstructions as well as the axial source images.

Patient studies were evaluated for their diagnostic value. An experienced neuroradiologist, blinded to both the results of the contrast angiographic examination as well as the underlying MR data acquisition strategy, analyzed the three image sets on the basis of presence of disease. No attempt was made to grade the stenoses on the MR images. Analysis was limited to the common carotid, the carotid bifurcation, the proximal internal (ICA) and external (ECA) carotid arteries, as well as the proximal vertebral arteries (V1, V2).

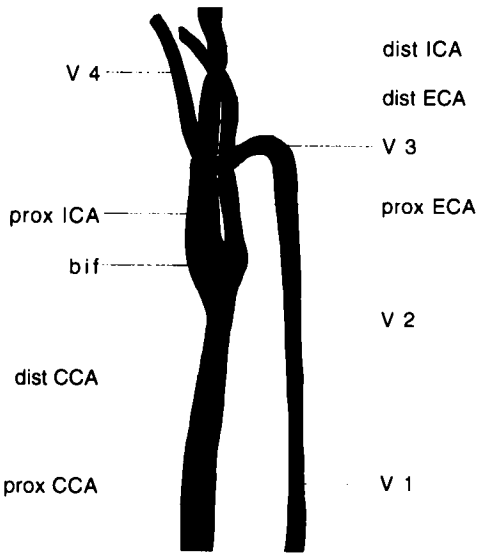

FIG. 1. Schematic illustration of the evaluated carotid and vertebral segments. CCA, common carotid artery; bif, carotid bifurcation; ICA, cervical internal carotid artery; ECA, external carotid artery; V1–4, vertebral segments 1–4.

Statistical Analysis

Vessel SNRs, vessel-to-background CNR, and SI ratios of conventional and EPI-based acquisitions were compared with a paired Student t test. For these purposes, SIs of the left and right CCAs were averaged.

The qualitative performance of each technique in the volunteer study was determined by calculating the mean number of visualized vessel segments for each subject and statistically compared on a segment-for-segment basis with respect to the two evaluated acquisition strategies, using a nonparametric Wilcoxon rank test.

RESULTS

Normal Subjects

The 12 volunteers and 3 patients tolerated the MRA studies well. The conventional 3D PC data were acquired in 459 s. With the 3D EPI technique, data collection for the same imaging volume comprising the same number of axial images was accomplished in merely 32 s. Accordingly, the EPI strategy shortened data acquisition times compared with the conventional technique by a factor of ~15.

SNRs were significantly higher for conventional images (mean 37.3 ± 5.7) than EPI images (mean 5.7 ± 1.0) ($p < 0.0001$). Vessel-to-background SI ratios, on the other hand, were significantly higher for the EPI images (mean 132 ± 82 vs. 89 ± 26) ($p < 0.03$). CNRs again favored conventional images (36 ± 4 vs. 6 ± 0.7) ($p < 0.0001$).

The CCA, the carotid bifurcation, as well as the proximal portion of the ECA and ICA were well visualized with both conventional and EPI PC acquisitions. In fact, all five proximal carotid segments (proximal and distal CCA, carotid bifurcation, proximal ICA and ECA) were seen in all 12 normal subjects on both the conventional as well as the EPI image sets (Figs. 2 and 3). The proximal vertebral segments V1 and V2 were similarly well seen with both techniques. In a single subject, only one vertebral artery was visualized with both data sets, reflecting an anatomic anomaly. In only one subject, a V2 segment seen on conventional images was not visible on the EPI set (Fig. 3).

The remaining distal segments of the ECA, the

2a,b

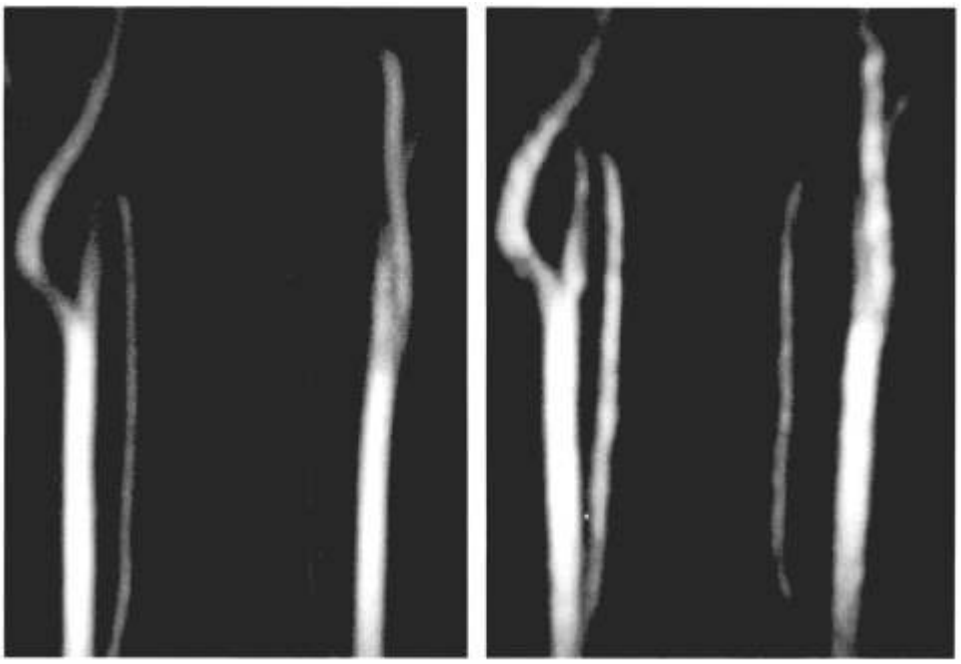

FIG. 2. Three-dimensional phase contrast MR angiograms of the carotid and vertebral arteries in a normal volunteer, based on 64 axial 2.5 mm sections. Coronal reprojections of the conventional data **(a)** acquired over 459 s and echo planar data **(b)** collected over merely 32 s. The proximal carotid and vertebral systems are seen on both images to equal advantage.

ICA, as well as the vertebral arteries were not fully visualized with either technique. On conventional images, the distal ICA was seen 83% of the time, the distal ECA segments in only 42%. The performance of conventional 3D PC was, however, superior to that of the EPI PC acquisition (Figs. 2 and 3). EPI images permitted adequate assessment of merely 29% of the distal ICA and none of the distal ECA segments. Similarly, visualization of the distal vertebral segments V3 and V4 was less complete on EPI images (V3 = 25%, V4 = 0%) compared with conventionally acquired image sets (V3 = 70%, V4 = 21%). In all five of these distal vessel segments, conventional 3D PC outperformed EPI PC with regard to arterial visibility ($p < 0.05$).

Patients

In all three evaluated subjects, minor atherosclerotic changes were seen throughout the carotid and vertebral vessels. In two of the patients examined, invasive angiography revealed a unilateral stenosis of the proximal ICA extending into the carotid bulb, severe (90%) in one case and moderate (75%) in the second. In the former, a concomitant moderate (75%) stenosis involved the proximal ECA. In the third patient, the right vertebral artery was proximally occluded. Both ICA stenoses and the vertebral artery occlusion were prospectively identified on both the conventional and the EPI 3D PC image sets (Fig. 4).

DISCUSSION

The employed 3D EPI data collection strategy significantly shortened imaging times, while maintaining image quality sufficient for the assessment of the proximal carotid system. With use of a 3D PC MRA acquisition, arterial vessels of the neck were imaged within a 15 cm wide volume, consisting of 60 axial 2.5 mm sections, in merely 32 s.

In contrast to conventional MRI techniques, which require a separate MR experiment for the acquisition of each line in *k*-space, EPI collects multiple *k*-space lines following a single RF excitation (16,17). Several EPI MRA sequences have been developed (11–13,18). Using a GRE-based EPI MRA

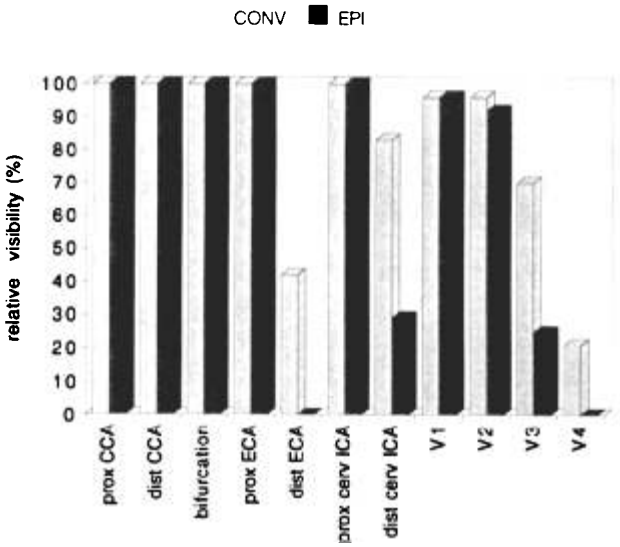

FIG. 3. Graphic illustration of the qualitative visibility data. The relative visibility is plotted for each of the evaluated vessel segments for both conventional and echo planar techniques. See Fig. 1 for abbreviations.

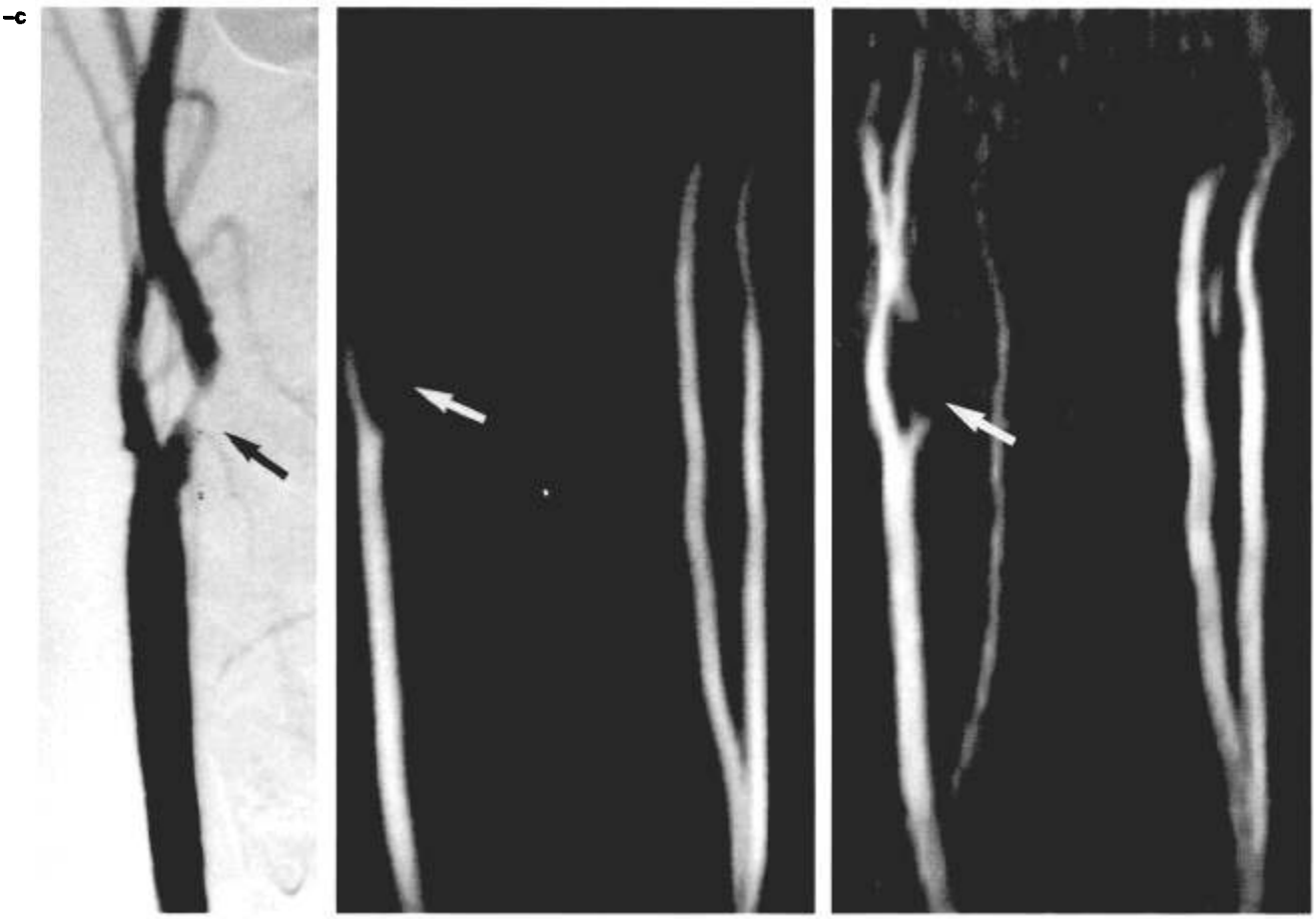

FIG. 4. Selective digital subtraction angiogram **(a)** of the right carotid artery reveals a high grade lesion involving the proximal internal carotid artery (arrow). Mild disease is seen in the proximal external carotid artery. The lesion (arrows) is identified on both the conventional 3D phase contrast MR angiogram **(b)** as well as on the echo planar angiogram **(c)**.

sequence, Goldberg et al. (12) reported diagnostic images of the hepatic and portal venous systems. Careful analysis of the employed imaging parameters, revealing a rather limited in-plane resolution of 1.6 × 3.2 mm, points to limitations of the EPI approach with regard to image quality.

Since data for EPI images are collected over a free induction decay, data lines acquired much beyond the tissue T2* decay time will contain little signal. The resulting compromise in the high spatial frequency image information leads to poor edge definition, with the inability to delineate small structures such as carotid or vertebral arteries (19). The short T2* decay time of blood within vessels as well as the surrounding fat limits achievable image resolution if all *k*-lines are collected after a single RF pulse (single shot EPI). Further limitations with regard to the length of the GE train following an RF pulse arise from increases of flow-induced spin dephasing artifacts, resulting in intravascular flow voids (17). It is thus highly desirable to reduce the GE train length and thus the data acquisition window by limiting the number of acquired data lines per RF pulse (20). This can be achieved by employing partial *k*-space coverage. Some oversampling (25%), however, is required to keep flow estimation errors within acceptable bounds (21). A more effective shortening of the GE train can be accomplished by collecting the image data not in a single but in several packages referred to as "shots" (20). To avoid off-resonance ghosting, multishot EPI data are collected in a *k*-space interleaved fashion (14,22). Due to the shortening of the data acquisition time, the high spatial frequency image information is now collected within the T2* time, translating into improved edge detection and conspicuity of small vascular structures (20).

To warrant adequate visualization of the carotid and vertebral vascular systems, data acquisition of a 2D plane of the 3D *k*-space was divided into eight shots. Eight shots were chosen based on preliminary sequence optimization. Breaking up the gradient train into eight shots results in a pronounced shortening of the echo train length and thus the effective TE, rendering an in-plane resolution of 1 × 1 mm. In fact, the TE of 9.4 ms with EPI was not much longer than the 7.2 ms TE of the conventional 3D PC sequence. At the same time, shortening the

TE reduces motion-induced dephasing artifacts, translating into more homogeneous intravascular signal (11). The multishot EPI approach used in this study thus combines high image quality with ultrafast data acquisition.

Each of the two fundamental approaches to vascular MR, TOF and PC, offers theoretical advantages and disadvantages (23). Currently the TOF technique is the one favored for evaluation of the carotid arteries by most institutions (23). Due to the better depiction of small vessels with PC MRA, some authors maintain that both techniques are complementary. At this time, no conclusive data are available with regard to the imaging performance of the two techniques in the carotid arteries. For the depiction of the intracranial vascularity as well as for renal arteries, the PC technique has been shown to be superior to TOF (23,24). This has largely been attributed to in-plane flow saturation phenomena inherent to the TOF technique. One of the more important factors favoring TOF over PC for imaging of the carotid arteries is the length of the imaging time (23). Depending on whether flow is encoded in one or all three planes, PC data acquisition exceeds TOF imaging times by a factor of 2 or 4, respectively. Beyond increasing imaging cost, prolongation of the imaging time augments the potential for motion artifacts. The ensuing degradation of image quality might render the study nondiagnostic or might even mimic pathology such as fibromuscular dysplasia in areas of normal vascular morphology (25). With ultrafast EPI data collection techniques, absolute differences in imaging times become considerably less relevant. Hence, the advantages of PC imaging, including better background suppression, reduced intravoxel dephasing, reduced sensitivity to spin saturation, and adjustable flow sensitivity (6,9,15,26–28), appear to outweigh those of TOF. Furthermore, the directional component inherent to PC imaging permits easy differentiation of venous from arterial signal, obviating the need for spatial saturation pulses. To enable a valid quantitative and qualitative comparison of the conventional and EPI MRA image sets, the conventional reference MRA exam was also performed with the PC technique. This study design was chosen to accentuate differences in image quality related to patient motion during data acquisition.

Multiplanar cross-sectional acquisition techniques may be based on either 2D or 3D Fourier transforms. While 2D approaches generally require less imaging time and are less sensitive to spin saturation phenomena, there are several advantages to 3D imaging. It allows acquisition of very thin sections with minimal interslice cross-talk (5). The smaller voxel size reduces partial voluming errors and decreases intravoxel dephasing. These characteristics are of particular value in the assessment of the carotid bifurcation (29). Since SNR increases as the square root of the number of phase encodings perpendicular to the imaging plane (30), 3D imaging is also characterized by higher SNRs than 2D acquisitions. In view of this advantage, the implementation of the 3D Fourier transform into SNR-limited echo planar acquisition strategies, as first described by Cohen and Rohan (31), represents a natural next step.

Another important reason favoring the use of 3D *k*-space acquisitions for EPI MRA acquisitions reflects the pulsatility of the arterial system. The acquisition time for a 2D EPI image is considerably shorter than the length of an RR interval. To ensure that data collection coincides with antegrade systolic flow, either image acquisition needs to be gated to systole, or, as suggested by Goldberg et al. (12), multiple images can be acquired in the same location. Both solutions result in a significant lengthening of imaging times, diminishing the speed advantage inherent to EPI data acquisition strategies. On the other hand, 3D EPI data sets are collected over a period exceeding the length of several cardiac cycles, hence representing flow averaged over that same period. This approach allows one to take full advantage of EPI's ultrafast acquisition speed. For echo planar MRA of the pulsatile arterial system, a 3D strategy thus appears clearly preferable.

The higher vessel-to-background SI ratios with EPI, reflecting higher intravascular signal on the magnitude-weighted EPI phase images, compensate to some degree for the increased noise inherent to EPI. Similar observations were made on 2D TOF EPI images (12). SNR and CNR of EPI, however, remained significantly below the levels achieved with the conventional acquisition, due to the rather high level of noise in the EPI images. The latter reflects differences in voxel bandwidth, increasing noise by a factor of ~2.5, and the use of a high bandwidth analog receiver for the EPI acquisition, increasing noise by another factor of 2. Improvements in receiver technology might alleviate this difference considerably in the near future.

Despite the significantly poorer SNR and CNR levels, qualitative assessment of this initial implementation of a 3D PC EPI sequence was encouraging. The entire CCA, the carotid bifurcation, as well as the proximal portions of the cervical ICA and ECA were well seen in all 12 subjects evaluated. The patient studies confirm that pathologic changes in the proximal carotid system are similarly well depicted. The achieved spatial resolution even permitted visualization of the proximal vertebral arteries. Congenital absence of one vertebral artery in 1 of the 12 volunteers was documented, as well as the proximal occlusion of a vertebral artery in one of the patients evaluated.

Significant differences in the performance of conventional and EPI 3D PC acquisitions became ap-

parent in the evaluation of the more distal vessel regions. The distal portion of the cervical ICA, the ECA, as well as the V3 and V4 segments of the vertebral tree were less well seen with EPI than with conventional technique. Incomplete visualization of these segments even on conventional image sets suggests that the poor performance of 3D PC EPI with regard to the distal arterial segments reflects limitations inherent to 3D imaging in general as well as those particular to EPI. The latter include the significantly lower SNR and CNR levels, as well as the longer effective TE, resulting in more spin dephasing (29,32). Optimization of the selection pulses might further reduce the TE of 3D PC EPI, mitigating these effects.

The employed 3D EPI PC imaging parameters were chosen to ensure a compromise between short data acquisition time and adequate image quality. A benchmark of 30 s seemed desirable not to exceed. It is quite conceivable, however, that changes in the individual data acquisition parameters associated with an increase in data acquisition time might improve image quality. Thus, doubling the number of excitations might result in a significant increase of image quality. The associated doubling of imaging time to 64 s would still represent a vast improvement compared with the conventional PC MRA techniques.

More dramatic improvements in the performance of 3D PC EPI can, however, be expected from the implementation of other measures, benefiting both conventional and EPI acquisitions. Intravascular SI could be enhanced on the magnitude-weighted PC images by the administration of extracellular contrast agents (33). Increased venous signal would remain of no consequence, owing to the directional component of the PC method. Spatially variable flip angles or TONE pulses have been demonstrated to effectively reduce spin saturation at no expense to imaging time (34,35). Another approach centers on the use of multiple thin slab 3D acquisitions, as first suggested by Parker et al. (36). These have proved useful in reducing the loss in CNR associated with saturation of blood (37). The lengthening of the examination time would not dramatically affect the absolute EPI data acquisition time. The stair step or venetian blind appearance on the projection images, reflecting the nonuniform section profiles, might represent a greater challenge. Recently, Tkach et al. (26) demonstrated improved depiction of small peripheral carotid segments on conventionally acquired 3D TOF MIP images, by varying the TR temporally over the course of the acquisition of each complete section-encoding loop. The potential of this technique with echo planar acquisitions still needs to be explored.

In conclusion, we have presented initial experience with a 3D echo planar strategy for imaging of the carotid and vertebral arteries in merely 32 s. In its current form, the performance of 3D PC EPI remains inferior to that of conventional MRA. With technical refinements, however, this approach may evolve into a cost-efficient, noninvasive, and sufficiently accurate screening test in the assessment of atherosclerotic disease in the carotid arteries.

Acknowledgment: This work was supported by SNF grant 32-2549.88 and KWF grant 2194.1

REFERENCES

1. NASCET collaborators. Beneficial effect of carotid endarterectomy in symptomatic patients with high-grade carotid stenosis. *N Engl J Med* 1991;325:445–53.
2. Hankey GJ, Warlow CP, Sellar RJ. Cerebral angiographic risk in mild cerebrovascular disease. *Stroke* 1990;21:209–22.
3. Polak JF, Bajakian RL, O'Leary DH, Anderson MR, Donaldson MC, Jolesz FA. Detection of internal carotid artery stenosis: comparison of MR angiography, color Doppler sonography, and arteriography. *Radiology* 1992;182:35–40.
4. Huston J, Lewis BD, Wiebers DO, Meyer FB, Riederer SJ, Weaver AL. Carotid artery: prospective blinded comparison of two-dimensional time-of-flight MR angiography with conventional angiography and duplex US. *Radiology* 1993;186: 339–44.
5. Wagle WA, Dumoulin CL, Souza SP, Cline HE. 3DFT MR angiography of carotid and basilar arteries. *AJNR* 1989;10: 911–9.
6. Applegate GR, Talagala SL, Applegate LJ. MR angiography of the head and neck: value of two-dimensional phase-contrast projection technique. *AJR* 1992;159:369–74.
7. Laster RJ, Acker JD, Halford HH, Nauert TC. Assessment of MR angiography versus arteriography for evaluation of cervical carotid bifurcation disease. *AJNR* 1993;14:681–8.
8. Saloner D, Anderson CM, Rapp J, Reilly L, Gooding GAW. Is X-ray angiography a reliable gold standard for assessing MRA of the carotid bifurcation? Correlation with endarterectomy specimens. In: *Book of abstracts: Society of Magnetic Resonance*. San Francisco: Society of Magnetic Resonance, 1994:949.
9. Chao PW, Goldberg H, Dumoulin CL, Wehrli FW. Comparison of time of flight versus phase contrast techniques: visualization of the intra and extracerebral carotid artery. In: *Book of abstracts: Society of Magnetic Resonance in Medicine*. Amsterdam: Society of Magnetic Resonance in Medicine, 1989:165.
10. Mansfield P. Multi-planar image formation using NMR spin echoes. *J Phys* [C] 1977;10:L55–8.
11. McKinnon GC. Interleaved echo planar phase contrast angiography. *Magn Res Med* 1994;31:682–5.
12. Goldberg MA, Yucel EK, Saini S, Hahn PF, Kaufman JA, Cohen MS. MR angiography of the portal and hepatic venous systems: preliminary experience with echoplanar imaging. *AJR* 1993;160:35–40.
13. Wielopolski PA, Edelman RR. Ultrafast, high resolution 3D STAR MR angiography using interleaved segmented echo planar readouts. In: *Book of abstracts: Society of Magnetic Resonance*. San Francisco: Society of Magnetic Resonance, 1994:948.
14. McKinnon GC. Ultrafast interleaved gradient-echo-planar imaging on a standard scanner. *Magn Res Med* 1993;30:609–16.
15. Edelman RR. MR angiography: present and future. *AJR* 1993;161:1–11.
16. Stehling MK, Mansfield P, Ordidge RJ, et al. Echo-planar imaging of the human fetus in utero. *Magn Res Med* 1990; 13:314–8.

17. Davis CP, McKinnon GC, Debatin JF, et al. Normal heart: evaluation with echo-planar MR imaging. *Radiology* 1994; 191:691–6.
18. Holtz DJ, Debatin JF, Unterweger M, Wildermuth S, Leung DA, von Schulthess GK. Phase-contrast evaluation of venous flow-augmentation: effect on ultrafast MR-venography of the calf. In: *Book of abstracts: Society of Magnetic Resonance*. San Francisco: Society of Magnetic Resonance, 1994:957.
19. Farzaneh F, Riederer SJ, Pelc NJ. Analysis of T2 limitations and off-resonance effects on spatial resolution and artifacts in echo planar imaging. *Magn Res Med* 1990;14:123–39.
20. Wetter DR, McKinnon GC, Debatin JF, von Schulthess GK. Single and multiple shot technique cardiac echo planar MR imaging: comparison of. *Radiology* 1994;194:765–70.
21. McKinnon GC, Debatin JF, von Schulthess GK. On the optimum parameters for rapid phase contrast flow measurements. In: *Book of abstracts: Society of Magnetic Resonance*. San Francisco: Society of Magnetic Resonance, 1994:148.
22. Butts K, Riederer SJ, Ehman RL, Thompson RM, Jack CR. Interleaved echo planar imaging on a standard MRI system. *Magn Res Med* 1994;31:67–72.
23. Huston J, Ehman RL. Comparison of time-of-flight and phase-contrast MR neuroangiographic techniques. *Radiographics* 1993;13:5–19.
24. Debatin JF, Ting RH, Wegmuller H, et al. Renal artery blood flow: quantitation with phase-contrast MR imaging with and without breath holding. *Radiology* 1994;190:371–8.
25. Heiserman JE, Drayer BP, Fram EK, Keller PJ. MR angiography of cervical fibromuscular dysplasia. *AJNR* 1992;13: 1454–7.
26. Tkach JA, Lin W, Duda JJ Jr, Haacke EM, Masaryk TJ. Optimizing three-dimensional time-of-flight MR angiography with variable repetition time. *Radiology* 1994;1991:805–11.
27. Debatin JF, Spritzer CE, Grist TM, et al. Imaging of the renal arteries: value of MR angiography. *AJR* 1991;157:981–90.
28. Spritzer CE, Pelc NJ, Lee JN, Evans AJ, Sostman HD, Riederer SJ. Rapid MR imaging of blood flow with a phase-sensitive, limited-flip-angle, gradient recalled pulse sequence: preliminary experience. *Radiology* 1990;176:255–62.
29. Masaryk AM, Ross JS, Di Cello MC, Modic MT, Paranandi L, Masaryk TJ. 3DFT MR angiography of the carotid bifurcation: potential and limitations as a screening examination. *Radiology* 1991;179:797–804.
30. Wehrli FW, McFall JR, Newton TH. Parameters determining the appearance of NMR images. In: Newton TH, Potts DG, ed. *Modern neuroradiology*. San Anselmo: Clavadel, 1983:87–9.
31. Cohen MS, Rohan ML. 3D volume imaging with instant scan. In: *Book of abstracts: Society of Magnetic Resonance in Medicine*. Amsterdam: Society of Magnetic Resonance in Medicine, 1989:831.
32. Patel MR, Klufas RA, Kim D, Edelman RR, Kent KC. MR angiography of the carotid bifurcation: artifacts and limitations. *AJR* 1994;162:1431–7.
33. Prince MR, Yucel EK, Kaufman JA, Harrison DC, Geller SC. Dynamic gadolinium-enhanced three-dimensional abdominal MR arteriography. *J Magn Res Imag* 1993;3:877–81.
34. Purdy DE, Cadena G, Laub G. Variable-tip-angle slab selection for improved three-dimensional MR angiography. In: *Book of abstracts: Society of Magnetic Resonance in Medicine*. Berlin: Society of Magnetic Resonance in Medicine, 1992:882.
35. Nägele T, Klose U, Grodd W, Petersen D, Tintera J. The effects of linearly increasing flip angles on 3D inflow MR angiography. *Magn Res Med* 1994;31:561–6.
36. Parker DL, Yuan C, Blatter DD. MR angiography by multiple thin slab 3D acquisition. *Magn Res Med* 1991;17:434–51.
37. Blatter DD, Parker DL, Robison RO. Cerebral MR angiography with multiple overlapping thin slab acquisition. Part I. Quantitative analysis of vessel visibility. *Radiology* 1991; 179:805–11.